Design Method of Ball Mill by Discrete Element Method

Sumitomo Chemical Co., Ltd.

Process & Production Technology Center

Makio KIMURA
Masayuki NARUMI
Tomonari KOBAYASHI

The grinding rate of gibbsite in tumbling and rocking ball mills using fins was well correlated with the specific impact energy of the balls calculated from Discrete Element Method simulation.

This relationship was successfully used for the scale-up of a rocking ball mill, and the optimum design and operating conditions for the rocking ball mill could be estimated by the specific impact energy of the balls calculated by a computer simulation.

Introduction

In recent years the demands for functional inorganic materials have been expanding in a variety of fields, such as display materials, energy, automobiles and semiconductors. Since the performance of these inorganic materials greatly affects the performance of the products in the fields mentioned above, various compositions and manufacturing conditions are explored to establish optimum performance. In the manufacturing of functional inorganic materials, "grinding" can be cited as an important unit operation. Grinding operations do not simply grind materials. They are used for the purpose of mixing, transporting, promoting physical properties and heat transfer, preprocessing for recovery of valuable materials, expression of functions and the like.

A ball mill is one kind of grinding machine, and it is a device in which media balls and solid materials (the materials to be ground) are placed in a container. The materials are ground by moving the container. Because the structure of ball mills is simple and it is easy to operate, and so they are widely used.

However, designing these devices and selecting conditions depend in many ways on empirical knowledge, and they have not been sufficiently systematized. Therefore, to scale-up these devices is not always easy, and collecting data requires a lot of effort and cost.

On the other hand, with the recent improvements in computational techniques that have accompanied increased performance in computers in recent years, it has become possible to analyze many fields using computer simulations. In the field of powder technology, Cundall et al.[1] have proposed a simulation method targeting the motion of particles, and it has had a great amount of success in application to the analysis of various phenomena. This method is called the discrete element method (DEM), and it is a method that tracks the motion of individual particles based on equations of motion. Research on ball motion in mills using the discrete element method has been proposed by Mishra et al.[2] and Yanagi et al.[3] So far, reports on analyses simulating three-dimensional analysis and complex liner shapes,[4, 5] and research on mill power consumption [6, 7] have been published.

However, most of them are concerned with the simulation of only the balls' motion in a mill. In actual grinding, the balls are not alone in the mill, but rather are present with the solid materials. To have a more accurate simulation of the grinding behavior, we must also simulate the motion of the solid materials, but because the number of particles for the solid material is so large, it is impossible to track all of the particles included in the solid materials with current computer capabilities. Therefore, we must model the presence of the solid materials and introduce this into the simulation. Observing the ball motion in experiments, the surfaces

of the balls are in a state where they are covered with the solid materials. It appears as if balls coated with the solid materials are moving. Therefore, Kano et al.[8] have simulated changing the coefficients of friction of the balls and have discovered that the coefficients of friction on the ball motion are extremely effective. It has been reported that if a suitable coefficient of friction is selected for each solid material from these results, the ball motion can be reproduced with good precision.

In addition, the collision frequency of the balls, the kinetic energy of the balls, the contact force between balls, the trajectory of ball motion and the like can be obtained from the simulation of ball motion. This information is an important factor for controlling the changes in characteristics of the solid materials in the grinding process. Kano et al.[8] found that it was the impact energy of the balls that has a large effect on the grinding.

Rocking mills (ball mills where the pot is rocked while rotating) are used to prevent adhesion and solidification of the solid materials on the pot during grinding, and to scale-up these has been investigated. However, collection of data has required effort as mentioned earlier. Therefore, we focused on the discrete element method, and carried out joint research with Professor Saito and Senior Assistant Professor Kano at Tohoku University for the purpose of establishing a method for scale-up using rocking ball mill simulations.

In this paper, we will introduce the results of predictions of grinding phenomena in rocking mills with fin plates and rocking mills using a combination of discrete element method simulation analysis and experimental investigations as well as the scale-up method and the optimum design method of these mills.

Simulations

1. Discrete Element Method

The discrete element method is a method that models contact forces such as the elastic repulsive force and frictional force working between particles that are in contact with each other and performs a numerical analysis of the motion of the individual particles operated on by the forces of contact based on the equations of motion for each. In a ball mill, the collisions between two balls or a ball and the mill wall are expressed by a Voigt model that expresses elastic spring (spring coefficient K) where elastic and inelastic properties of the objects are introduced between the points of contact as

(a) Compressive force   (b) Shear force
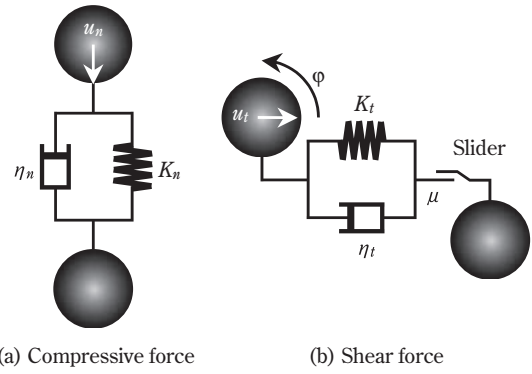
Fig. 1   Model of interactive forces between two balls

shown in **Fig. 1** and the viscosity dashpot (damping coefficient η). In addition, a friction slider (coefficient of friction μ) is introduced into the tangential component of the interactive force to express frictional interaction attendant to ball contact.

The forces of contact between balls are given by the following equation as the compressive forces in the normal direction (F_n) and the shear forces in the tangential direction (F_t).

$$F_n = K_n \Delta u_n + \eta_n \frac{\Delta u_n}{\Delta t} \tag{Eq. 1}$$

$$F_t = \min\left\{ \mu F_n,\ K_t \Delta(u_t + r\varphi) + \eta_t \frac{\Delta(u_t + r\varphi)}{\Delta t} \right\} \tag{Eq. 2}$$

Here, u and φ are the relative displacement and the relative angular displacement, respectively, between the two particles we are focusing on, and k, η, μ and r are the spring coefficient damping coefficient, coefficient of friction and the radius of the balls.

The spring coefficient K_n in the normal direction is given by the following equation using the Young's modulus E of the ball and the mill wall, and Poisson's ratio v and using the Hertz theory of elastic contact. The subscripts i, j and w indicate the balls i and j and the mill wall.

$$K_{nij} = \frac{4}{3\pi} \left[\frac{1}{\delta_i + \delta_j} \right] \sqrt{\frac{r_i r_j}{r_i + r_j}} \tag{Eq. 3}$$

$$K_{niw} = \frac{4}{3\pi} \sqrt{r_i}\ \frac{1}{\delta_i + \delta_w} \tag{Eq. 4}$$

$$\delta_i = \frac{1 - v_i^2}{E_i \pi} \tag{Eq. 5}$$

$$\delta_j = \frac{1 - v_j^2}{E_j \pi} \tag{Eq. 6}$$

$$\delta_w = \frac{1 - v_w^2}{E_w \pi} \tag{Eq. 7}$$

The spring coefficient in the tangential direction K_s can be obtained based on the defining equation for the Lame constant shown in (Eq. 8), which shows the relationship between the shear ratio and Young's modulus for the substance.

$$K_s = \frac{K_n}{2(1+v)} \qquad \text{(Eq. 8)}$$

In a vibration equation with a single degree of freedom having the elastic spring and viscosity dashpot,

$$\eta = 2\sqrt{m \cdot K} \qquad \text{(Eq. 9)}$$

is when the damping is the fastest. Cundall[1] has proposed considering the relationship in (Eq. 9) where the rebounding phenomenon that arises from collisions among the elements is made to dampen as quickly as possible with η determined. Simulations in this paper employed the same method of determination.

The physical constants used in these calculations are given in **Table 1**.

Table 1	Physical properties for DEM simulation	
Young's modulus	[Pa]	3.5×10^8
Poisson's ratio	[−]	0.23
Frictional coefficient	[−]	0.8
Density of balls	[kg/m^3]	3452
Time step	[μs]	10.0

In a discrete element method simulation of the inside of a ball mill, the coefficient of friction of the balls is the most important factor, and it has been reported that the spring coefficient and damping coefficient calculated from Young's modulus and Poisson's ratio do not have a large effect on the ball motion.[9] There is correlation between the coefficient of friction and grinding, and with gibbsite powder, it has been reported to be roughly 0.3 – 0.8,[8] so we used 0.8 here.

2. Impact Energy of Balls

Using the discrete element method, it is possible to obtain the collision frequency of the balls , the kinetic energy of the balls the contact force between balls, the trajectories of motion and other information about the movements of the balls inside the ball mill either temporally or spatially. As mentioned above, Kano et al.[8] found the specific impact energy of the balls (E_W)

defined by (Eq. 10) has an especially large effect on the grinding.

$$E_W = \frac{1}{W} \sum_{j=1}^{n} \frac{1}{2} m v_j^2 \qquad \text{(Eq. 10)}$$

where, W is the weight of the solid materials, n the number of collisions, m the mass of a ball and v_j the relative velocity between two colliding balls or a ball colliding against the mill wall.

Experiment

Gibbsite powder (Al(OH)$_3$, with an average particle diameter of 30 – 50 μm, Sumitomo Chemical Co. Ltd., CHP-340S) was used for the solid material.

Fig. 2 shows a schematic diagram of the rocking mill (Aichi Electric Co., Ltd.) used in this study. The rocking mill has the axis of tumbling rotation of a typical tumbling mill and an axis of rocking rotation perpendicular to this. It is a grinding device that is capable of rocking the pot while it is rotating. Three fins are provided on the inside of the mill, and we used two types of mill where the capacity of the pot was 60 L and 300 L.
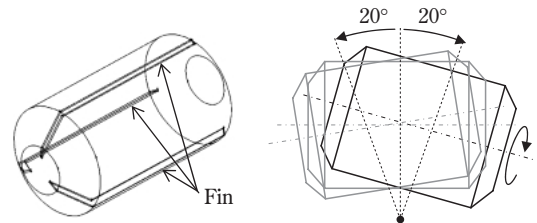
| Fig. 2 | Schematic diagram of the rocking ball mill |

The mill was filled with 15 mm nylon coated iron balls, and the rotational speed N of the mill was varied in a range from 40%–100% using the critical rotational speed N_c defined by (Eq. 11) as a reference. The critical rotational speed N_c is the limiting speed where the balls move together with the mill wall due to the centrifugal force.

$$N_c = \frac{60}{\pi} \sqrt{\frac{g}{2D_m}} \qquad \text{(Eq. 11)}$$

where, D_m is the inside diameter of the mill, and g is gravitational acceleration. Grinding was carried out for 180 minutes. At specific times during that period, the mill was stopped, and small volume samples were

Table 2	Mill configuration and experimental conditions			

			60L mill	300L mill
Pot diameter	[mm]		344	590
Pot depth	[mm]		690	1185
Height of fin	[mm]		20	40
Swing speed	[spm]*		12	12
Critical rotational speed	[rpm]		72	55
Number of balls	[–]		7870	39120
Weight of gibbsite	[kg]		10.2	51

＊ spm : frequency of swing per minute

collected. The diameter of the gibbsite powder was measured using a Master Sizer 2000 (Sysmex Corporation). Details of the experimental conditions are given in **Table 2**.

Results and Discussion

1. Effects of Fins on Ball Motion in the Mill

To predict ball mill grinding behavior using the discrete element method, we must first be able to reproduce the balls' motion in the ball mill using simulations.

Kano et al.[8] have made it clear that it is possible to reproduce the ball motion when the solid material is also present in a tumbling ball mill without fins by providing a suitable coefficient of friction for the balls and carrying out simulations. That suitable coefficient of friction is 0.17 for the balls alone, and roughly in the range of $0.3-0.8$ when gibbsite is coexistent.

In this paper, we carried out simulations varying the coefficient of friction for the balls in a range of
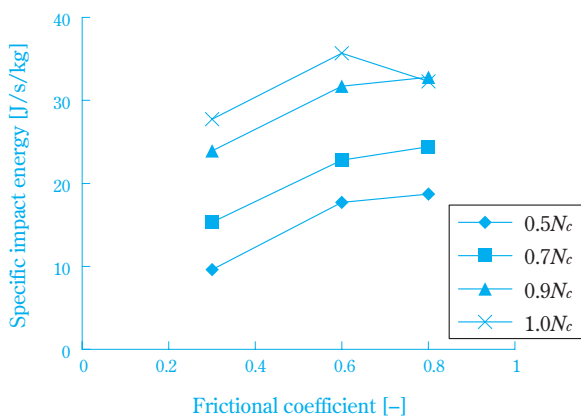
Fig. 3	Relation between specific impact energy and frictional coefficient of 60L tumbling mill without fin
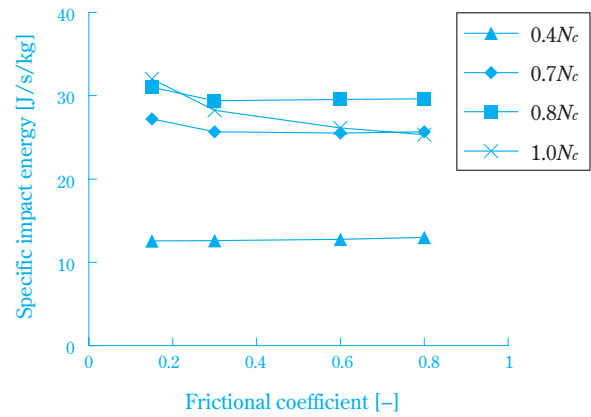
Fig. 4	Relation between specific impact energy and frictional coefficient of 60L tumbling mill with fin

$0.15-0.8$, and by comparing Ew obtained as a result, we confirmed the effects of the coefficient of friction on ball motion. The relationship between the coefficient of friction and Ew for a 60 L tumbling mill without fins is shown in **Fig. 3**, and that for a 60 L tumbling mill with fins is shown in **Fig. 4**.

We can see that when the coefficient of friction changes without fins, there is also a large change in Ew. On the other hand, when the tumbling rotational speed is 1.0 Nc when there are fins, there is a tendency for Ew to change with changes in the coefficient of friction, but when the tumbling rotational speed is 0.8 Nc or less, Ew has substantially the same value. With the mill that does not have fins, the height of the balls lifted up by the mill wall increases with a larger coefficient of friction, so even at the same tumbling rotational speed, different behavior appears. However, we can assume that when the mill is provided with fins, the balls are lifted up by the fins, so the effect of the coefficient of friction becomes extremely small. Thus, we can assume that with a tumbling mill that has fins, the ball motion in the mill is substantially the same regardless of the presence or absence of the material being ground and with a tumbling rotational speed smaller than the critical speed of rotation.

Therefore, we carried out observational experiments where the motion of the balls in the mill with fins was made visible and compared it with the simulation results. **Table 3** gives the results for a tumbling mill, and **Table 4** gives the results for a rocking mill.

In these experiments, a clear acrylic plate was used for the mill cover to make visual observations possible. When the ball motion had sufficiently stabilized after

Table 3 Snapshots of the motion of balls in the tumbling mill (Experiment and DEM simulation results)

starting up the mill, we filmed the ball motion with a video camera under conditions with a tumbling speed of rotation of 0.4 N_c – 1.0 N_c. When the gibbsite powder was introduced, it became difficult to visualize the ball behavior inside the mill because the gibbsite powder adhered to the clear acrylic plate, so we have only shown the results when the mill was filled with balls only. On the other hand, the results for a simulation carried out with a coefficient of friction of 0.8 are given. The ball motion at all of the conditions in these results agrees well with the simulation results, and we were able to confirm that the ball behavior could be reproduced in simulations.

2. Relationship between Grinding Rate and Tumbling Rotational Speed (60 L Tumbling and Rocking Mills)

Fig. 5 shows the normalized median diameter (D_t/D_0) of the gibbsite powder when using the 60 L tumbling mill as a function of grinding period time depending on the tumbling rotational speed. Here, D_0 is the initial median particle diameter and D_t is the median particle diameter after t seconds of grinding.

Table 4 Snapshots of the motion of balls in the rocking mill (Experiment and DEM simulation results)

Fig. 5 Relation between normalized median diameter of the gibbsite and grinding time at 60L tumbling mill

We can see that the normalized median diameter is reduced exponentially with time. This process can be approximated by (Eq. 12) so as to be shown as a solid line.

$$\frac{D_t - D_l}{D_0 - D_l} = \exp\left(-K_p t^{0.5}\right) \qquad \text{(Eq. 12)}$$

where, K_p is defined as the grinding rate. In addition, D_l denotes the median diameter at the grinding limit, and $D_l/D_0 = 0.135$ from the experimental.

In the same manner, **Fig. 6** shows the normalized median diameter (D_t/D_0) of the gibbsite powder when using the 60 L rocking mill as a function of the grinding period time depending on the tumbling rotational speed.
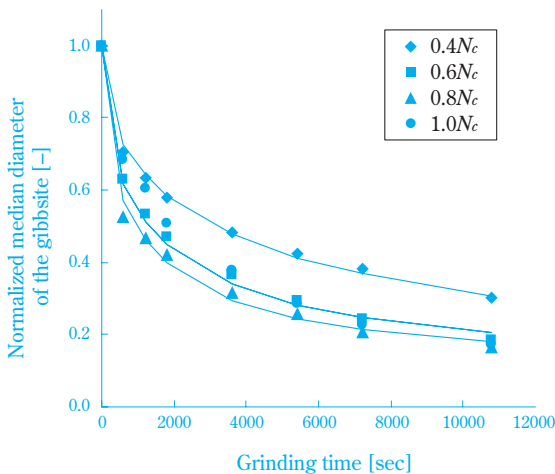
Fig. 6 Relation between normalized median diameter of the gibbsite and grinding time at 60L rocking mill

Fig. 7 shows the relationship between K_p defined in (Eq. 12) and the relative tumbling rotational speed (N/N_c). We can see that at a tumbling rotational speed of 0.8 N_c, the tumbling mill and the rocking mill have a K_p of substantially the same value. In addition, K_p in the rocking mill increases with an increase in the tumbling rotational speed, and an extremely large value was exhibited at 0.8 N_c. A trend where it dropped rapidly when the tumbling rotational speed was 1.0 N_c could be seen. The reason for this can be assumed to be that the potential energy of the balls that are lifted up increases with an increase in the tumbling rotational speed, and K_p increases along with this. Furthermore, when the tumbling rotational speed reaches 1.0 N_c, the centrifugal force becomes large, but the balls adhere to the wall surface and make a state where they rotate together, so the collisions between the balls are reduced dramatically, and K_p suddenly drops off.
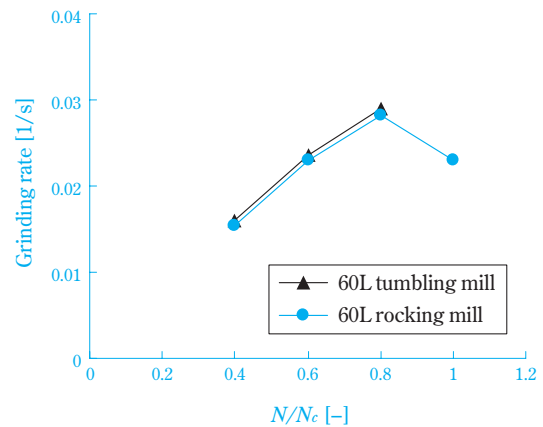
Fig. 7 Relation between grinding rate and relative rotational speed

3. Relationship between Impact Energy of Balls and Tumbling Rotational Speed (60 L Tumbling and Rocking Mills)

Fig. 8 shows the relationship between the specific impact energy of the balls (E_w) calculated from the simulation results and the relative tumbling rotational speed (N/N_c). With the tumbling mill, there was an extremely large value in the neighborhood of 0.8 N_c, and with the rocking mill, there was a trend that exhibited an extremely large value in the neighborhood of 1.0 N_c. The reason for this can be assumed to be that, as with the relationship between K_p and N/N_c, the potential energy of the balls increases with an increase in the tumbling rotational speed, and because of this,
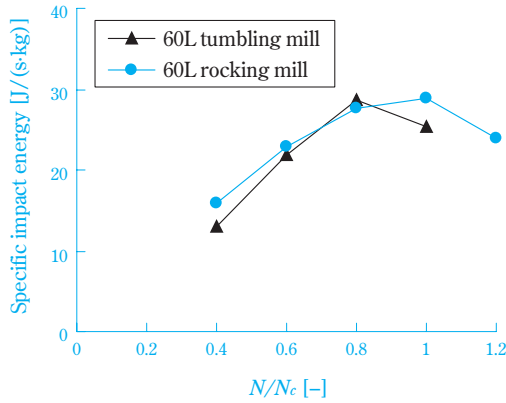
Fig. 8 Relation between specific impact energy and relative rotational speed

Ew also increases. Furthermore, when the tumbling rotational speed gets to the neighborhood of 1.0 N_c, the balls adhere to the wall surface because of the centrifugal force, so there is a remarkable drop in the collisions between balls, and *Ew* is reduced.

4. Relationship between Grinding Rate and Impact Energy of Balls

When we compared the relationship (Fig. 8) between *Ew* for the balls calculated by carrying out a simulation of ball motion under the same conditions as the grinding experiments using the discrete element method and N/N_c as well as the relationship (Fig. 7) between K_p and N/N_c, we found that there was a roughly similar pattern at rotational speeds less than the critical rotational speed.

Therefore, the relationship between K_p at rotational speeds less than the critical rotational speed and *Ew* found using the simulation is shown in **Fig. 9**.
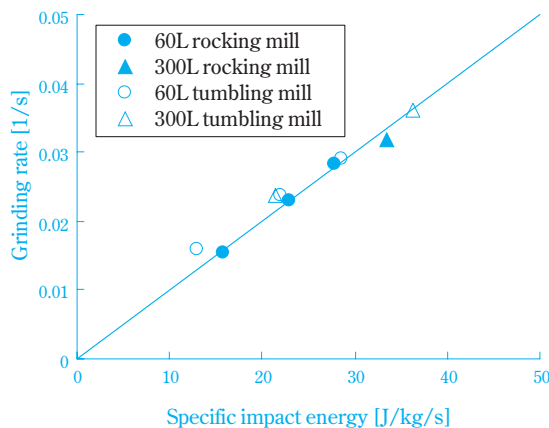
Fig. 9 Relation between grinding rate and specific impact energy

The plot in this figure was drawn to include the results of K_p and *Ew* in a 300 L tumbling mill and a 300 L rocking mill also.

A good correlative relationship was found in the points that were plotted, and this relationship arises regardless of the capacity of the mill and the presence or absence of rocking.

If we use this relationship, we can find K_p by finding *Ew* using the discrete element method, and by substituting K_p into (Eq. 12), we can predict the temporal changes in the median particle diameter for actual grinding.

5. Scale-up Method for Tumbling Mills and Rocking Mills

A correlative relationship was found between K_p found by experiment and *Ew* calculated from the simulations regardless of the mill capacity and whether or not there was rocking, so it is possible to increase the scale of tumbling mills and rocking mills using this relationship.

The scale-up procedure is given in the following.

(1) The optimum coefficient of friction for the balls is established, and the actual ball behavior is reproduced by simulation.

(2) Several experiments and simulations are carried out for each type of material to be ground in a small-scale tumbling mill.

(3) The correlative relationship between K_p according to the type of solid materials and *Ew* is found.

(4) Simulations are carried out with scale-up tumbling mills and rocking mills, and *Ew* for the balls is calculated.

(5) K_p during grinding with a rocking mill is predicted using the correlative relationship in (3).

If the scale-up method by combining experiments and simulations above is used, it is possible to reduce the frequency of the experiments carried out up to now by trial and error, and this can contribute to a reduction in the effort and costs required for scale-up.

6. Optimization of Design Conditions for Ball Mills

If simulations are used it is possible to freely change various conditions such as the shape of the mill. It is possible to carry out optimization of design conditions for tumbling mills and rocking mills by carrying out simulations with various conditions and compare *Ew* calculated from the results. Here we will give an example of examining the effects of ball diameter and the height of fins.

(1) Effects of Ball Diameter

Fig. 10 shows the relationship between the ball diameter and Ew at a tumbling rotational speed of 0.8 N_c. The number of balls was set so as to have the same weight of balls (**Table 5**), and the weight of gibbsite was fixed at 10.2 kg.
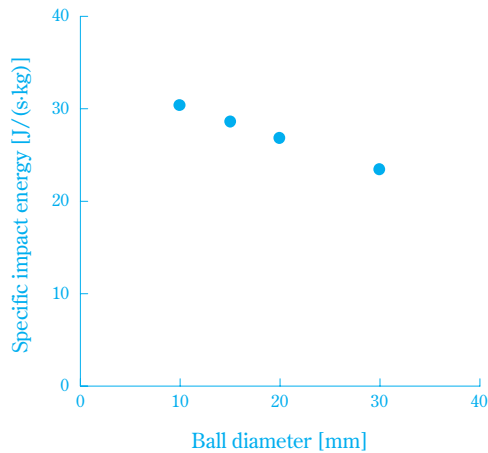
Fig. 10   Relation between ball diameter and specific impact energy

Table 5   Calculation conditions

Ball diameter	Number of balls
10mm	26560
15mm	7870
20mm	3320
30mm	984

There was a tendency for Ew to be larger with smaller diameter balls, and it was estimated that K_p would also show the same tendency. We can assume that at conditions where the weight of the balls and the weight of gibbsite were the same, the number of balls increased as diameter of the balls became smaller and the number of collisions increased, so we had this kind of trend.

(2) Effects of Fin Height

Fig. 11 shows the relationship between fin height and Ew under the conditions of tumbling rotational speeds of 0.6 N_c and 0.8 N_c. We can see that Ew becomes somewhat higher with the installation of the fins. However, we can see that even if the height of the fins is increased, no large difference was found in the value for Ew. In the case of 0.8 N_c, the trend was for Ew to reach a maximum when the fin height was 5 mm.
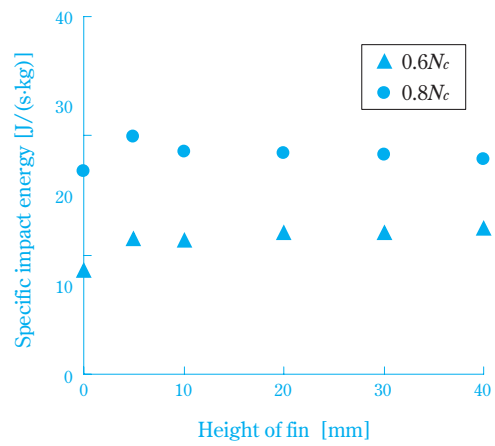
Fig. 11   Relation between the height of fin and specific impact energy

Conclusion

We have established a method where reproduction and prediction of the grinding phenomena in rocking mills are possible with good precision by combining simulation based on the discrete element method and experimental investigation. At rotational speeds below the critical rotational speed, a good correlative relationship is clearly established between the grinding rate and the specific impact energy of the balls regardless of the presence or absence of rocking and the size of the mill. If this relationship is used it is possible to scale-up with a minimum frequency of experiments and find the optimum operating conditions and design conditions. Moving forward, we would like to work on parallel development for grinding equipment such as agitated bead mills and vibrating mills. If this can be achieved, it will be possible to select types of grinding equipment using this method, and we can assume that higher levels of grinding process development and increased speed will be achieved. Furthermore, since the same kind of approach can be applied to the mechanochemical reactions, we would also like to develop it in that direction.

Acknowledgements

References

1) P.A. Cundall and O.D.L. Strack, *Geotechnique*, **29**, 47 (1979).

2) B. K. Mishra and R. K. Rajamani, *KONA*, **8**, 92 (1990).

3) H. Ryu, H. Hashimoto, F. Saito and R.Watanabe, *Shigen-to-Sozai*, **108**, 549 (1992).

4) P. W. Cleary, *Minerals Engineering*, **11**, 1061 (1998).

5) R. K. Rajamani, B. K. Mishra, R. Venugopal and A.Datta, *Powder Technology*, **109**, 105 (2000).

6) A.Datta, B. K. Mishra, and R. K. Rajamani, *Canadian Metallurgical Quarterly*, **38**, 133 (1999).

7) M. A. van Nierop, G. Glover, A. L. Hinde and M. H. Moys, *International Journal of Mineral Processing*, **61**, 77 (2001).

8) J. Kano, N. Chujo and F. Saito, *Advanced Powder Technology*, **8**, 39 (1997).

9) The Society of Powder Technology, Japan: *Funtai Simulation Nyumon* [*Introduction to Granular Simulation*], p.74, Sangyo Tosho, (1998).

PROFILE

Makio KIMURA

Sumitomo Chemical Co., Ltd.
Process & Production Technology Center
Senior Research Associate

Tomonari KOBAYASHI

Sumitomo Chemical Co., Ltd.
Process & Production Technology Center
Research Associate

Masayuki NARUMI

Sumitomo Chemical Co., Ltd.
Process & Production Technology Center
Research Associate